

# White light emission from Dy<sup>3+</sup>-doped LiLuF<sub>4</sub> single crystal grown by Bridgman method\*

DONG Yan-ming (董艳明)<sup>1</sup>, XIA Hai-ping (夏海平)<sup>1\*\*</sup>, FU Li (符立)<sup>1</sup>, LI Shan-shan (李珊珊)<sup>1</sup>, GU Xue-mei (谷雪梅)<sup>1</sup>, ZHANG Jian-li (章践立)<sup>1</sup>, WANG Dong-jie (王冬杰)<sup>1</sup>, ZHANG Yue-pin (张约品)<sup>1</sup>, JIANG Hao-chuan (江浩川)<sup>2</sup>, and CHEN Bao-jiu (陈宝玖)<sup>3</sup>

1. Key Laboratory of Photo-electronic Materials, Ningbo University, Ningbo 315211, China

2. Ningbo Institute of Materials Technology and Engineering, the Chinese Academy of Sciences, Ningbo 315211, China

3. Department of Physics, Dalian Maritime University, Dalian 116026, China

(Received 2 April 2014)

©Tianjin University of Technology and Springer-Verlag Berlin Heidelberg 2014

Lithium lutetium fluoride (LiLuF<sub>4</sub>) single crystals doped with different Dy<sup>3+</sup> ion concentrations were grown by Bridgman method. The Judd-Ofelt (J-O) strength parameters ( $\Omega_2$ ,  $\Omega_4$ ,  $\Omega_6$ ) of Dy<sup>3+</sup> in LiLuF<sub>4</sub> crystal are calculated according to the measured absorption spectra and the J-O theory, by which the asymmetry of the Dy<sup>3+</sup>:LiLuF<sub>4</sub> single crystal and the possibility of attaining stimulated emission from <sup>4</sup>F<sub>9/2</sub> level are analyzed. The capability of the Dy<sup>3+</sup>:LiLuF<sub>4</sub> crystal in generating white light by simultaneous blue and yellow emissions under excitation with ultraviolet light is produced. The effects of excitation wavelength and doping concentration on chromaticity coordinates and photoluminescence intensity are also investigated. Favorable CIE coordinates,  $x=0.3193$  and  $y=0.3493$ , can be obtained for Dy<sup>3+</sup> ion in 2.701% molar doping concentration under excitation of 350 nm.

**Document code:** A **Article ID:** 1673-1905(2014)04-0262-4

**DOI** 10.1007/s11801-014-4052-4

Recently, much attention has been paid on Dy<sup>3+</sup>-doped materials for their characteristics of ~483 nm (<sup>4</sup>F<sub>9/2</sub>→<sup>6</sup>H<sub>15/2</sub>) blue and ~574 nm (<sup>4</sup>F<sub>9/2</sub>→<sup>6</sup>H<sub>13/2</sub>) yellow emissions for the possibility of obtaining white light, which can be potentially applied for LEDs<sup>[1]</sup>. Zhang et al<sup>[2]</sup> firstly reported the white light emission from Dy<sup>3+</sup>-doped borate glass. After that, some Dy<sup>3+</sup>-doped glasses for white light emission, such as silicate<sup>[3]</sup>, borosilicate<sup>[4]</sup> and alumina silicate<sup>[5]</sup>, have been developed for their advantages of homogeneous light emitting, simple manufacture procedure, low production cost and good thermal stability. However, the poor mechanical and thermal properties, and low emission efficiency of the glasses made them difficult for the practical applications in optical devices. So far, white light emissions and mid-IR light emission from some Dy<sup>3+</sup>-doped single crystals have been reported<sup>[6,7]</sup>. However, there are few reports on preparation and optical properties of LiLuF<sub>4</sub> single crystal doped with Dy<sup>3+</sup> ions. LiLuF<sub>4</sub> is similar to LiYF<sub>4</sub>, which crystallizes in a scheelite structure. They share a congruent melting behavior and present good optical quality. Compared with LiYF<sub>4</sub>, LiLuF<sub>4</sub> crystal has the advantages of lower up-conversion loss and laser threshold, which can improve the laser efficiency. LiLuF<sub>4</sub> crystals also have other advantages of good resistance to optical damage,

no thermally induced birefringence and the output of linearly polarized laser.

In this letter, we report the growth of Dy<sup>3+</sup>-doped LiLuF<sub>4</sub> single crystal by Bridgman method and demonstrate the capability of generating white light by simultaneous yellow and blue emissions of phosphorescent centers under excitation of ultraviolet light.

Dy<sup>3+</sup>-doped LiLuF<sub>4</sub> single crystals with the molar composition of 50.5LiF-(49.5-x)LuF<sub>3</sub>-xDyF<sub>3</sub>, where  $x=0.5\%$ , 1.0%, 2.0% and 3.0%, were prepared by the Bridgman method. Detailed process for the crystal growth was described in Ref.[8]. Fig.1 shows the photo of the grown Dy<sup>3+</sup>:LiLuF<sub>4</sub> single crystal with a size of 10 mm×75 mm. Along the growth direction, a small pale opaque matter of approximately several centimeters in length at the top of the crystal is observed, corresponding to the final portion of the melt-to-freeze transition. The small pale opaque matter is the eliquation layer, which results from excessive LiF in the starting materials. Small pieces of the grown crystals were cut and well polished to a thickness of 2.3 mm for the optical measurement. X-ray diffraction (XRD) patterns of the crystals were recorded using an XD-98X diffractometer (XD-3, Beijing) to investigate the crystals' structure. Lambda 950 UV/VIS/NIR spectrophotometer was used to record

\* This work has been supported by the National Natural Science Foundation of China (Nos.51272109 and 11374044), the Natural Science Foundation of Ningbo city (No.201401A6105016), and K.C. Wong Magna Fund in Ningbo University.

\*\* E-mail: hpxcm@nbu.edu.cn

the absorption spectra. The fluorescence and the excitation spectra were recorded by a fluorophotometer (Cary Eclipse, American). The concentrations of Dy<sup>3+</sup> ions in LiLuF<sub>4</sub> single crystals were measured by inductively coupled plasma atomic emission spectroscopy (ICP-AES, PerkinElmer Inc., Optima3000). The same experimental conditions were maintained to get comparable results. All these measurements were carried out at room temperature.

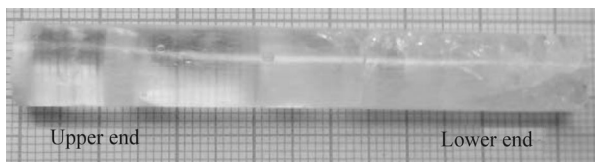


**Fig.1** The photo of the as grown Dy<sup>3+</sup>-doped LiLuF<sub>4</sub> single crystal

Fig.2 shows the powder XRD pattern of the 0.998% Dy<sup>3+</sup> single-doped LiLuF<sub>4</sub> crystals, which is used to identify the crystal phase of the samples. The lattice parameters calculated from the XRD pattern are  $a=b=0.5130$ ,  $c=1.0562$  and also illustrated in Fig.2. By comparing the peak positions with those in JCPD No.27-1251 of pure LiLuF<sub>4</sub>, one can conclude that the grown crystal is a single tetragonal phase. The similar XRD patterns were obtained for 0.471%, 0.998%, 1.958% and 2.701% (molar concentration) Dy<sup>3+</sup> singly-doped LiLuF<sub>4</sub> crystal samples, suggesting that all the samples have been crystallized into the pure tetragonal phase. The measured concentrations of Dy<sup>3+</sup> ions in the as-grown LiLuF<sub>4</sub> single crystal are shown in Tab.1.

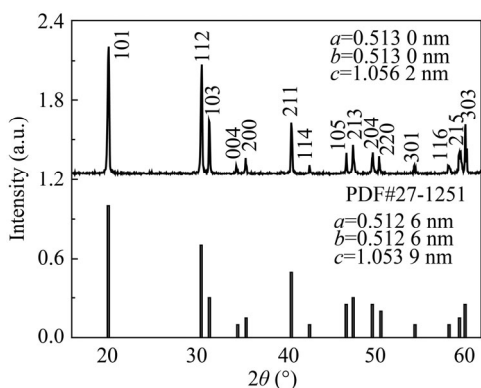


**Fig.2** Powder XRD pattern of Dy<sup>3+</sup>-doped LiLuF<sub>4</sub> single crystal and standard card of LiLuF<sub>4</sub> (JCPD No.27-1251)

**Tab.1** Concentration of Dy<sup>3+</sup> ion in the LiLuF<sub>4</sub> single crystal (molar ratio)

| Sample           | i      | ii     | iii    | iv     |
|------------------|--------|--------|--------|--------|
| Dy <sup>3+</sup> | 0.471% | 0.998% | 1.958% | 2.701% |

Absorption spectra of Dy<sup>3+</sup> singly-doped LiLuF<sub>4</sub> single crystals in the wavelength range of 300—700 nm and the absorption bands of Dy<sup>3+</sup> corresponding to the transitions starting from the ground state to the higher levels

are shown in Fig.3. Obvious absorptions around 325 nm (<sup>6</sup>H<sub>15/2</sub> → <sup>4</sup>M<sub>17/2</sub>), 350 nm (<sup>6</sup>H<sub>15/2</sub> → <sup>6</sup>P<sub>7/2</sub>), 364 nm (<sup>6</sup>H<sub>15/2</sub> → <sup>6</sup>P<sub>5/2</sub>), and 387 nm (<sup>6</sup>H<sub>15/2</sub> → <sup>4</sup>I<sub>13/2</sub>) of the Dy<sup>3+</sup>-doped crystal indicate that the crystal can be efficiently excited by UV light.

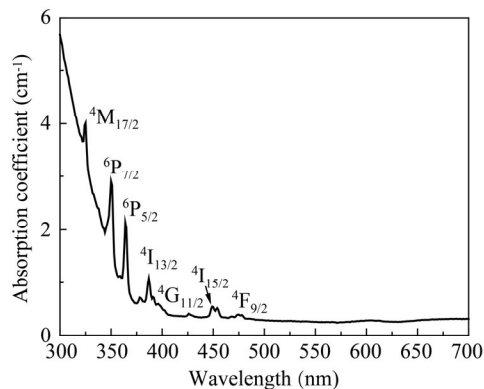


**Fig.3** Absorption spectrum of Dy<sup>3+</sup> singly-doped LiLuF<sub>4</sub> single crystal

Based on the absorption spectrum, the optical parameters of 0.998% Dy<sup>3+</sup>: LiLuF<sub>4</sub> sample are obtained by applying J-O theory. The spontaneous emission probabilities and the radiative branching ratios for the transitions from the <sup>4</sup>F<sub>9/2</sub> state to the lower ones have been estimated using the calculated intensity parameters and the reduced matrix elements reported by C. K. Jayasankar<sup>[9]</sup>. Detailed process for the calculation was described in Ref.[10]. The calculated J-O parameters  $\Omega_2$ ,  $\Omega_4$ ,  $\Omega_6$ , spontaneous emission probabilities  $A$  and radiative branching ratios  $\beta$  for the <sup>4</sup>F<sub>9/2</sub> emitting level of Dy<sup>3+</sup>:LiLuF<sub>4</sub> crystals are listed in Tab.2. The calculated J-O parameters are compared with those reported for other crystals activated with Dy<sup>3+</sup> and listed in Tab.3.

**Tab.2** Calculated spontaneous emission probabilities  $A$  and radiative branching ratios  $\beta$  for the <sup>4</sup>F<sub>9/2</sub> emitting level of Dy<sup>3+</sup> in LiLuF<sub>4</sub>

| Final state                    | $A$ (s <sup>-1</sup> ) | $\beta$ |
|--------------------------------|------------------------|---------|
| <sup>6</sup> F <sub>1/2</sub>  | 0.035                  | 0.000   |
| <sup>6</sup> F <sub>3/2</sub>  | 0.064                  | 0.000   |
| <sup>6</sup> F <sub>5/2</sub>  | 2.320                  | 0.004   |
| <sup>6</sup> F <sub>7/2</sub>  | 20.646                 | 0.035   |
| <sup>6</sup> H <sub>5/2</sub>  | 1.722                  | 0.003   |
| <sup>6</sup> H <sub>7/2</sub>  | 10.459                 | 0.018   |
| <sup>6</sup> F <sub>9/2</sub>  | 71.132                 | 0.122   |
| <sup>6</sup> F <sub>11/2</sub> | 20.444                 | 0.035   |
| <sup>6</sup> H <sub>9/2</sub>  | 8.153                  | 0.014   |
| <sup>6</sup> H <sub>11/2</sub> | 26.524                 | 0.045   |
| <sup>6</sup> H <sub>13/2</sub> | 291.948                | 0.500   |
| <sup>6</sup> H <sub>15/2</sub> | 130.655                | 0.224   |

Intensity parameters  
 $\Omega_2=2.14 \times 10^{-20} \text{ cm}^2$   
 $\Omega_4=0.94 \times 10^{-20} \text{ cm}^2$   
 $\Omega_6=1.87 \times 10^{-20} \text{ cm}^2$   
 $RMS=2.7 \times 10^{-7}$

The value of the branching ratio for  ${}^4F_{9/2} \rightarrow {}^6H_{13/2}$  transition is found to be maximum, which suggests that this transition could give a good rise to fluorescent action.

**Tab.3 Comparison between the intensity parameters of the developed compound and other Dy<sup>3+</sup>-activated crystals**

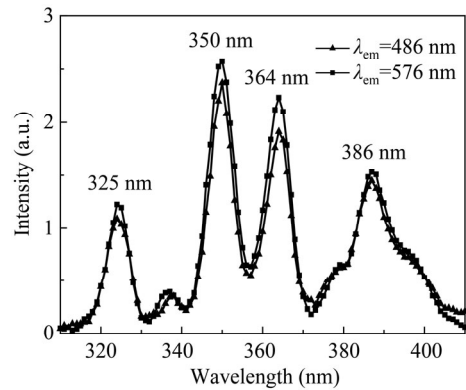
|  | $\Omega_2 (\times 10^{-20} \text{ cm}^2)$ | $\Omega_4 (\times 10^{-20} \text{ cm}^2)$ | $\Omega_6 (\times 10^{-20} \text{ cm}^2)$ | Reference |
|--|---|---|---|-----------|
| LiLuF <sub>4</sub>                               | 2.14                                      | 0.94                                      | 1.87                                      | This work |
| LiLuF <sub>4</sub>                               | 2.04                                      | 0.91                                      | 1.09                                      | [11]      |
| CaMoO <sub>4</sub>                               | 26.6                                      | 2.89                                      | 1.79                                      | [12]      |
| KY(WO <sub>4</sub> ) <sub>2</sub>                | 23.2                                      | 3.33                                      | 2.36                                      | [13]      |
| YAl <sub>3</sub> (BO <sub>3</sub> ) <sub>4</sub> | 10.8                                      | 2.05                                      | 3.28                                      | [14]      |

Generally, the J-O parameters provide an insight into the local structure and bonding in the neighbourhood of RE<sup>3+</sup> ions. In particular,  $\Omega_2$ , magnitude of structure/environment parameter, which depends on covalency of metal-ligand bond and also explains the symmetry in the vicinity of RE ion sites, is highly sensitive to local structure of the Dy<sup>3+</sup> ion. Lower magnitude of  $\Omega_2$  can suggest that the Dy<sup>3+</sup> ion site has higher asymmetry in the host matrix. The  $\Omega_4$  parameter is related to the bulk properties and  $\Omega_6$  is inversely related to the rigidity of host. In the obtained Dy<sup>3+</sup>:LiLuF<sub>4</sub> single crystal, the Dy<sup>3+</sup> ion takes the place of Lu<sup>3+</sup>, the asymmetry caused by the fact that the radius of the Dy<sup>3+</sup> ion is larger than that of the Lu<sup>3+</sup> ion when they are embedded together in the lattice explained the smaller values of  $\Omega_2$ . By the comparison of the J-O parameters of Dy<sup>3+</sup> ions in different hosts as shown in Tab.3, we could find that LiLuF<sub>4</sub> has the smallest degree of covalency between the Dy<sup>3+</sup> ions and the surrounding ligands and/or the highest symmetry of the coordination structure surrounding the Dy<sup>3+</sup> ions for it has the smallest values of  $\Omega_2$ . In the obtained Dy<sup>3+</sup>:LiLuF<sub>4</sub> single crystal, the Dy<sup>3+</sup> ion takes the place of Lu<sup>3+</sup>, the Dy<sup>3+</sup> ion is surrounded by six closed packed F<sup>-</sup> ions to form octahedron structure.

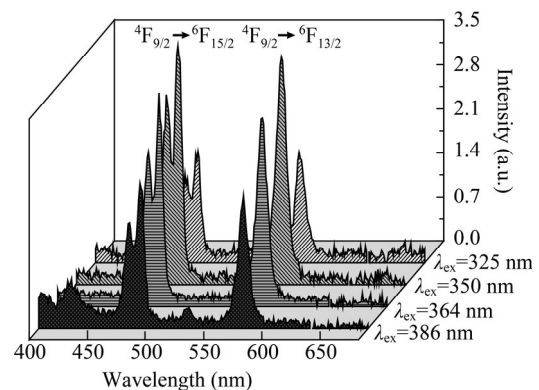
Generally, the Dy<sup>3+</sup> ion possesses energy levels for 486 nm and 576 nm emissions. Fig.4 shows the excitation spectra of the Dy<sup>3+</sup> doped LiLuF<sub>4</sub> crystal monitored at 486 nm and 576 nm, respectively. Two excitation spectral curves exhibit similar characteristic bands with excitation peaks located at 325 nm ( ${}^6H_{15/2} \rightarrow {}^4M_{17/2}$ ), 350 nm ( ${}^6H_{15/2} \rightarrow {}^6P_{7/2}$ ), 364 nm ( ${}^6H_{15/2} \rightarrow {}^6P_{5/2}$ ) and 386 nm ( ${}^6H_{15/2} \rightarrow {}^4I_{13/2}$ ). When monitored at 486 nm, the intensity is slightly weaker than that monitored at 576 nm.

Fig.5 shows the emission spectra of 0.998% Dy<sup>3+</sup> singly-doped LiLuF<sub>4</sub> single crystal under excitation of 325 nm, 350 nm, 364 nm and 388 nm, respectively. A blue band emission centered at 486 nm ( ${}^4F_{9/2} \rightarrow {}^6H_{15/2}$ ) and a yellow band centered at 576 nm ( ${}^4F_{9/2} \rightarrow {}^6H_{13/2}$ ) are observed in Fig.5. The emission intensities under 350 nm excitation are the strongest in the all spectra. It is indicated that the 350 nm light is the most effective one for exciting the obtained Dy<sup>3+</sup>:LiLuF<sub>4</sub> crystal. Fig.6 shows the effects of Dy<sup>3+</sup> doping concentration on the emission spectra in 400—680 nm of Dy<sup>3+</sup> singly-doped LiLuF<sub>4</sub>

crystal under 350 nm excitation. We can see from Fig.5 and Fig.6 that for all above UV light excitation, blue and yellow emissions can be simultaneously obtained. As the Dy<sup>3+</sup> ion molar doping concentration increases from 0.471% to 2.701%, the emission intensities at 461—500 nm and 553—595 nm bands gradually increase. The relative intensity changes between 480 nm and 573 nm are slight with various exciting wavelengths and Dy<sup>3+</sup> doping concentrations. As the doping concentration increases, the relative intensity between 480 nm and 573 nm increases first and then decreases after the 1.958% Dy<sup>3+</sup> doping concentration. Similar phenomena could be found in the emission spectra with different excitation wavelengths. It is indicated that the color of luminescence could be adjusted by varying the excitation wavelength and the doping concentration of Dy<sup>3+</sup>, and the quenching concentration of Dy<sup>3+</sup> in LiLuF<sub>4</sub> crystal reaches more than 2.701%.



**Fig.4 Excitation spectra of 0.998% Dy<sup>3+</sup> singly-doped LiLuF<sub>4</sub> single crystal monitored at 486 nm and 576 nm**



**Fig.5 Emission spectra in 400—680 nm band of 0.998% Dy<sup>3+</sup> singly-doped LiLuF<sub>4</sub> single crystal under 325 nm, 350 nm, 364 nm and 386 nm excitations**

The CIE chromaticity coordinates could be calculated from their corresponding emission spectra. Figs.7 and 8 show the CIE chromaticity coordinates of the 0.998% Dy<sup>3+</sup> singly-doped LiLuF<sub>4</sub> crystal under excitation of 325 nm, 350 nm, 364 nm and 388 nm, and the effects of Dy<sup>3+</sup> doping concentration on the CIE chromatic coordinate diagram under 350 nm excitation are also illustrated. It

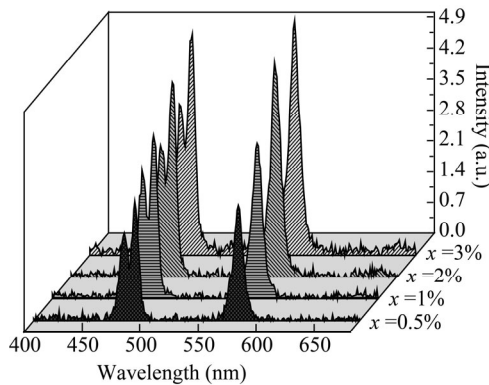


**Fig.6 Emission spectra in 400–680 nm band of 0.471%, 0.998%, 1.958% and 2.701% Dy<sup>3+</sup> singly-doped LiLuF<sub>4</sub> single crystals under 350 nm excitation**

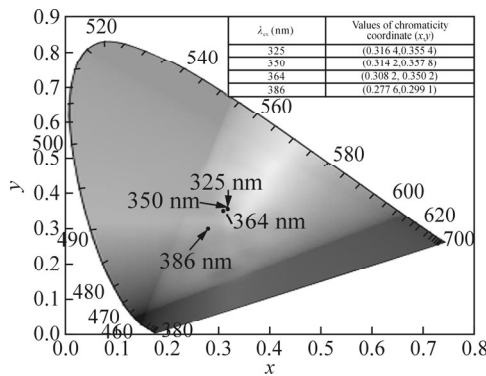


**Fig.7 CIE chromatic coordinate diagram of 0.998% Dy<sup>3+</sup> singly-doped LiLuF<sub>4</sub> single crystal under 325 nm, 350 nm, 364 nm and 386 nm excitations (The insert shows the comparison of the corresponding CIE chromaticity coordinates.)**

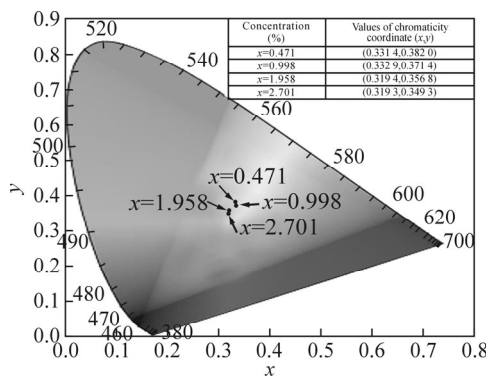


**Fig.8 CIE chromatic coordinate diagram of 0.471%, 0.998%, 1.958% and 2.701% Dy<sup>3+</sup> singly-doped LiLuF<sub>4</sub> single crystals under 350 nm excitation (The insert shows the comparison of the corresponding CIE chromaticity coordinates.)**

can be seen from Fig.7 that 386 nm is not an appropriate exciting wavelength for white light emission of 0.998%

Dy<sup>3+</sup> singly-doped LiLuF<sub>4</sub> single crystal due to bad coordinate of  $x=0.2776$  and  $y=0.2991$ . It can be seen from Fig.8 that a favorable chromatic coordinate of  $x=0.3193$ ,  $y=0.3493$  can be obtained for 2.701% Dy<sup>3+</sup>-doped sample.

Dy<sup>3+</sup>-doped LiLuF<sub>4</sub> single crystals with good quality and optical properties can be grown by Bridgman method. The Dy<sup>3+</sup> ion site has higher asymmetry in LiLuF<sub>4</sub> crystal due to the low magnitude of  $\Omega_2$ . The ultraviolet 350 nm can effectively excite the Dy<sup>3+</sup>-doped LiLuF<sub>4</sub> single crystal to emit the 486 nm blue and 576 nm yellow light waves. The color of luminescence can be adjusted by varying the excitation wavelength and the doping concentration of Dy<sup>3+</sup>. Favorable CIE coordinates,  $x=0.3193$  and  $y=0.3493$ , can be obtained for Dy<sup>3+</sup> ion in 2.701% doping concentration under excitation of 350 nm. Our results demonstrate that the crystal is a potential candidate for ultraviolet light-excited white light emission.

**References**

- [1] R. Zhang and X. Wang, *J. Alloys Compd.* **509**, 1197 (2011).
- [2] J. C. Zhang, C. Parent, G. le Flem and P. Hagenmuller, *J. Solid State Chem.* **93**, 17 (1991).
- [3] X. Y. Sun, S. M. Huang, X. S. Gong, Q. C. Gao, Z. P. Ye and C. Y. Cao, *J. Non-Cryst. Solids* **356**, 98 (2010).
- [4] Y. H. Lin, Z. L. Tang, Z. T. Zhang, J. Y. Zhang and Q. M. Chen, *Mater. Sci. Eng. B* **86**, 79 (2001).
- [5] S. M. Liu, G. L. Zhao, X. H. Lin, H. Ying, J. B. Liu, J. X. Wang and G. R. Han, *J. Solid State Chem.* **181**, 2725 (2008).
- [6] L. Tang, H. P. Xia, P. Y. Wang, J. T. Peng and H. C. Jiang, *Chin. Opt. Lett.* **11**, 061603 (2013).
- [7] L. F. Johnson and H. J. Guggenheim, *Appl. Phys. Lett.* **23**, 96 (1973).
- [8] H. P. Xia, J. H. Wang, X. L. Zeng, J. L. Zhang, Y. P. Zhang, J. Xu and Q. H. Nie, *J. Funct. Mater.* **36**, 238 (2005).
- [9] C. K. Jayasankar and E. Rukmini, *Physica B* **240**, 273 (1997).
- [10] J. Xiong, H. Y. Peng, P. C. Hu, Y. Hang and L. H. Zhang, *J. Phys. D: Appl. Phys.* **43**, 185402 (2010).
- [11] S. Bigotta, M. Tonelli, E. Cavalli and A. Belletti, *J. Lumin.* **130**, 13 (2010).
- [12] E. Cavalli, E. Bovero and A. Belletti, *J. Phys. Condens. Matter* **14**, 5221 (2002).
- [13] L. Macalik, J. Hanuza, B. Macalik, W. Ryba-Romanowski, S. Golab and A. Pietraszko, *J. Lumin.* **79**, 9 (1998).
- [14] R. Martínez Vázquez, R. Osellame, M. Marangoni, R. Ramponi, E. Diéguez, M. Ferrari and M. Mattarelli, *J. Phys.: Condens. Matter* **16**, 465 (2004).